Heat and Mass Transfer Analysis for the MHD Forced Convective Flow of a Nanofluid over a Slendering Stretching Sheet with Radiation in Porous Medium

K Suneetha[1], SM Ibrahim[2], GV Ramana Reddy[1], G Lorenzini[3]

[1]Department of Mathematics, K L University, Vaddeswaram, Guntur, India

[2]Department of Mathematics, GITAM University, Hyderabad, India

[3]Department of Engineering and Architecture, University of Parma, Parma, Italy

Abstract: Computational analysis of radiative heat and mass transfer of nanofluid over a slendering stretching sheet in porous medium with a non-even heat source and slip effects have been carried out in this article. The transformed equations of the flow model are solved by the Runge-Kutta scheme coupled with shooting method to depict the dimensionless velocity, temperature, and concentration at the boundary layer. Numerical computations are carried out and discussed for skin friction coefficient and local Nusselt number. We found an excellent agreement of the present results with the existed results under some special conditions. It is also found that the heat transfer performance is high in presence of velocity slip effect. Dimensionless skin-friction coefficient has decreased for increasing magnetic field, power law-index with velocity slip and wall thickness.

Keywords: Nano fluid, Thermal radiation, Porous medium, Slendering stretching sheet, MHD, Heat source

I. INTRODUCTION

In Recent days one of the principal challenges for the present and future industry is to meet the energy demands of the globe. This ever increasing demand is the key factor for the researchers to explore nanoparticles/nanofluids. The enhanced thermal performance of nanofluids/nanoparticles has vital importance in industrial fields such as power generation, micro- manufacturing, transportation, micro-electronics, thermal therapy for cancer treatment, pharmaceutical processes, chemical and metallurgical sectors, etc. In automobiles the appliance of nanofluids as coolants permit better size as well as positioning of the radiators this require less energy for improving resistance on the road. Ultra high performance cooling is necessary for many industrial technologies [1-3].

Choi [4,5] was the first to introduce the word nanofluid that represent the fluid in which nanoscale particles (diameter <50 nm) are suspended in the base fluid. With the rapid advances in nanotechnology, many inexpensive combinations of liquid/particles are now available. The base fluids used are usually water, ethylene glycol and oil. Recent research on nanofluids showed that nanoparticles changed the fluid characteristics because thermal conductivity of these particles was higher than convectional fluids. Nanoparticles are of great scientific interest as they are effectively a bridge between bulk materials and atomic or molecular structures.

The study of convective flow, heat and mass transfer in porous media has been an active field of research as it plays a crucial role in diverse applications, such as thermal insulation, extraction of crude oil and chemical catalytic reactors etc. Considerable work has been reported on flow and heat and mass transfer in porous media in [6–10].

Magnetohydrodynamics (MHD) boundary-layer flow of nanofluid and heat transfer over a stretching surface have received a lot of attention in the field of several industrial, scientific, and engineering applications in recent years. The comprehensive references on this topic can be found in the some review papers, for example, [11-21] investigated the effects of thermal radiation and magnetic field on the boundary layer flow of a nanofluid over a stretching surface. The flow in micro/nano systems such as hard disk drive, micro-pump, micro-valve and micronozzles is in slip transition regime, which is characterized by slip boundary at the wall. The liquids exhibiting boundary slip find its applications in technological problems. Therefore many boundary layer fluid flow problems have been revisited with slip boundary condition and different researchers have made significant contributions. Navier [22] suggested a slip boundary condition in terms of shear stress. Of late, the work of Navier was extended by many authors. GadelHak [23] established the fact that the micro-scale level the fluid flow is dominated by fluid surface interaction which belongs to slip flows regime, whereas the momentum equation remains to be Navier-Stokes equation. Slip flow past a stretching surface was analyzed by Andersson [24]. The combined effects of slip and convective boundary conditions on stagnation point flow of CNT suspended nanofluid over a stretching sheet was formulated by Akbar et al. [25]. Slip flow effects over MHD forced convective flow over a slendering stretching was studied by Anjali Devi and Prakash [26]. Ramana Reddy et al. [27] studied the thermophoresis and Brownian motion effects on MHD nanofluid flow over a slandering stretching sheet in presence of multiple slip effects. Kiran Kumar and Varma [28] examined the MHD boundary layer slip flow of nanofluid through porous medium over a slendering sheet. Sulochana and Sandeep [29] derived the dual solutions analysis on magnetichydrodynamic forced convective flow of a nanofluid over a slendering stretching sheet in the presence of porous medium. Multiple slip and cross diffusion effects on MHD Carreau-Casson fluid over a slendering sheet in presence of non-uniform heat source and sink was proposed by Raju et al. [30]. Multiple slip conditions on MHD boundary layer flow and heat transfer of a nanofluid past a permeable stretching sheet was investigated by Ibrahim and Shankar [31].

To the authors knowledge, no effort has been made still by the researchers to analyze heat and mass transfer over slendering sheet with heat source or sink and radiation. Hence by exploiting the above-cited studies we made an attempt to fulfill this gap. The considered flow equations are remodeled to a dimensionless form with the aid of suitable transformations. The equations are solved with the support of Runge-Kutta based shooting methods.

II. FORMULATION OF THE PROBLEM

Consider a steady two-dimensional, incompressible, laminar, hydro magnetic flow of a nano fluid over a stretching sheet with non-uniform thickness in porous medium. No-slip and Navier slip conditions are taken in to account. The sheet is along the x-axis direction and y-axis is normal to it as shown in Fig. 1. A variable magnetic field $B(x) = B_0(x+a)^{-(1-n)/2}$, $n \neq 1$ is applied to the flow, where B_0 is applied magnetic field strength and a is the physical parameter related to stretching sheet. Magnetic Reynolds number is assumed to be very small so that the induced magnetic field is neglected. A non-uniform permeability $K(x) = K_0(x+a)^{1-n}$, $n \neq 1$ along with the thermal radiation effect is taken into account. Viscous dissipation effect is neglected in this study. It is assumed that the sheet is stretched with the velocity $u_w(x) = u_0(x+a)^n$, $n \neq 1$ and the wall temperature $T_w(x) = T_\infty + T_0 (x+a)^{-(1-n)/2}$, $n \neq 1$. Since the sheet is non-uniform it is assumed that $y = A(x+a)^{(1-n)/2}$, $n \neq 1$, where A is the coefficient related to stretching sheet and chosen as a small constant to avoid the external pressure. At m=n=1 the problem refers flat stretching sheet case.
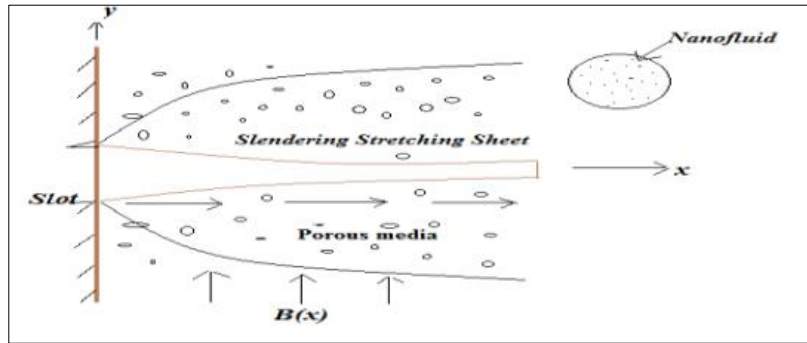
Fig. 1. Physical model and coordinate system.

As per the above assumptions the governing boundary layer equations are given as follows: [32,33]

$$\frac{\partial u}{\partial x} + \frac{\partial v}{\partial y} = 0 \tag{1}$$

$$u\frac{\partial u}{\partial x} + v\frac{\partial u}{\partial y} = \upsilon_f \frac{\partial^2 u}{\partial y^2} - \frac{\sigma B^2}{\rho_f}u - \frac{\upsilon_f}{K}u \tag{2}$$

$$u\frac{\partial T}{\partial x} + v\frac{\partial T}{\partial y} = \alpha \frac{\partial^2 T}{\partial y^2} - \frac{1}{\rho_f c_p}\frac{\partial q_r}{\partial y} + \tau\left[D_B\left(\frac{\partial C}{\partial y}\frac{\partial T}{\partial y}\right) + \left(\frac{D_T}{T_\infty}\right)\left(\frac{\partial T}{\partial y}\right)^2\right] + \frac{Q_s}{\rho_f c_p}\left(T - T_\infty\right) \tag{3}$$

$$u\frac{\partial C}{\partial x} + v\frac{\partial C}{\partial y} = D_m \frac{\partial^2 C}{\partial y^2} + \left(\frac{D_T}{T_\infty}\right)\left(\frac{\partial T}{\partial y}\right)^2 \tag{4}$$

The boundary conditions are as follows:

$$u(x,y) = u_w(x) + \delta_1^* \frac{\partial u}{\partial y}, v(x,y)=0, \ T(x,y) = T_w(x) + \delta_2^* \frac{\partial T}{\partial y}, \ C(x,y) = C_w(x) + \delta_3^* \frac{\partial C}{\partial y}, \ at \ y=0$$

$$u = 0, T = T_\infty, C = C_\infty \ \ as \ \ y \to \infty, \tag{5}$$

Where u and v are the velocity components along x and y directions respectively, ρf is the density of the fluid , v_f is the kinematic viscosity, σ is the electrical conductivity, T is the temperature of the fluid, k is the thermal conductivity, α is the diffusivity of the nano fluid, $(\rho c_p)_f$ is the specific heat capacitance , Q_s is coefficient of heat source/sink, δ_1^* is the dimensional velocity slip parameter and δ_2^* is dimensional temperature jump parameter, δ_3^* is dimensional concentration jump parameter, these are given by $\delta_1^* = \left(\frac{2-b}{b}\right)\xi_1(x+a)^{(1-n)/2}$ $\delta_2^* = \left(\frac{2-c}{c}\right)\xi_2(x+a)^{(1-n)/2}$,

$\delta_3^* = \left(\frac{2-d}{d}\right)\zeta_3(x+a)^{\frac{1-n}{2}}$, $\xi_2 = \left(\frac{2\lambda}{\lambda+1}\right)\frac{\xi_1}{\text{Pr}}$, $\zeta_3 = \left(\frac{2\lambda}{\lambda+1}\right)\frac{\zeta_2}{\text{Pr}}$, hear ξ_1, $\xi_{2 \ and} \ \xi_3$ are mean free paths and λ is the ratio of specific heats, b and c respectively indicates Maxwells reflection coefficient and thermal accommodation coefficient.

The radiative heat flux q_r under Rosseland approximation has the form

$$q_r = -\frac{4\sigma^*}{3k^*}\frac{\partial T^4}{\partial y}$$

Where σ^* is the Stefan-Boltzman constant and k^* is the mean absorption coefficient. The temperature differences within the flow are assumed to be sufficiently small such that T^4 may be expressed as a linear function of temperature. Expanding T^4 using Taylor series and neglecting order terms yields:

$$T^4 \cong 4T_\infty^3 T - 3T_\infty^4$$

To convert the governing equations in to set of nonlinear ordinary differential equations we now introducing the following similarity transformation [32].

$$\psi(x,y) = \left(\frac{2\upsilon_f u_0}{n+1}\right)^{0.5}(x+a)^{(n+1)/2}f(\eta), \text{n}\neq1, \ \eta = \left(\frac{(n+1)u_0}{2\upsilon_f}\right)^{0.5}(x+a)^{(n-1)/2}y, \ n\neq1$$

$$\theta(\eta) = (T-T_\infty)/(T_w(x)-T_\infty), \quad (6)$$

Where $\psi(x,y)$ is a stream function which satisfies the continuity equations (1) with

$$u = \frac{\partial \psi}{\partial y} \quad \text{and} \quad v = -\frac{\partial \psi}{\partial x} \qquad (7)$$

Using equations 6-7, equations 2-4 can be reduced in to the form

$$f''' - \left(\frac{2n}{n+1}\right)f'^2 + ff'' - (M+K_1)f' = 0 \quad (8)$$

$$\frac{1}{\text{Pr}}\left(1+\frac{4}{3}R\right)\theta'' - \left(\frac{1-n}{1+n}\right)f'\theta + f\theta' + Nb\theta'\phi' + Nt\theta'^2 + Q\theta = 0 \qquad (9)$$

$$\phi'' - Sc\left(\frac{1-n}{1+n}f'\phi - f\phi'\right) + \frac{Nt}{Nb}\theta'' = 0 \quad (10)$$

With the transformed boundary conditions

$$f(\gamma) = \gamma\left(\frac{1-n}{1+n}\right)[1+\delta_1 f''(0)], \ f'(\gamma) = [1+\delta_1 f''(0)]$$

$$\theta(\gamma) = [1+\delta_2\theta'(0)], \ \phi(\gamma) = [1+\delta_3\phi'(0)], \ f'(\infty)\to0, \ \theta(\infty)\to0, \ \phi(\infty)\to0 \ \text{n}\neq1 \qquad (11)$$

Where $\quad \gamma = A\left(\frac{(n+1)u_0}{2\upsilon_f}\right)^{0.5}\quad$, $\quad \delta_1 = \left(\frac{2-b}{b}\right)\xi_1\left(\frac{(n+1)u_0}{2\upsilon_f}\right)^{0.5}\quad \delta_2 = \left(\frac{2-c}{c}\right)\xi_2\left(\frac{(n+1)u_0}{2\upsilon_f}\right)^{0.5}\quad$,

$$\delta_2 = \left(\frac{2-d}{d}\right)\xi_3\left(\frac{(n+1)u_0}{2\upsilon_f}\right)^{0.5}$$

Here equations (8) and (10) are nonlinear ordinary differential equations in the domain $[\gamma,\delta]$.

For numerical computation we transformed the domain $[\gamma,\delta]$ in to $[0,\delta]$ by defining $F(\xi)=F(\eta-\gamma)=F(n)$ and $\theta(\xi)=\theta(\eta-\gamma)=\theta(\eta)$

Now the similarity equations become:

$$F''' - \left(\frac{2n}{n+1}\right)F'^2 + FF'' - (M+K)F' = 0 \qquad (12)$$

$$\frac{1}{\Pr}\left(1+\frac{4}{3}R\right)\Theta'' - \left(\frac{1-n}{1+n}\right)F'\Theta + F\Theta' + Nb\Theta'\Phi' + Nt\Theta'^{2} + Q\Theta = 0 \quad (13)$$

$$\Phi'' - Sc\left(\frac{1-n}{1+n}F'\Phi - F\Phi'\right) + \frac{Nt}{Nb}\Theta'' = 0 \quad (14)$$

With boundary conditions

$$F(0) = \gamma\left(\frac{1-n}{1+n}\right)[1+\delta_1 F''(0)], \; F'(0) = [1+\delta_1 F''(0)],$$

$$\Theta(0) = [1+\delta_2\Theta'(0)], \; \Phi(0) = [1+\delta_3\Phi(0)], \; F'(\infty) \to 0, \; \Theta(\infty) \to 0, \; \Phi(\infty) \to 0, \; n\neq 1 \quad (15)$$

Where the indicates the differentiation with respect to ξ. $M = 2\sigma B_0^2/\rho_f u_0(1+n)$ is he magnetic field parameter, $2v_f/k_0 u_0(1+n)$ is the porosity parameter, $\Pr = v_f/\alpha$ is the Prandtl number, $R = 4\sigma T_\infty^3/kk*$ is the radiation parameter,

$$Q = \frac{Q_s}{(n+1)\rho_f c_p}$$ is the heat source parameter, $$Sc = \frac{\upsilon_f}{D_B}$$ is the Schmidt number, n is the velocity power index

parameter, γ is the wall thickness parameter, δ_1 is the non-dimensional velocity slip parameter and δ_2 is the non-dimensional temperature jump parameter,

For engineering interest the shear coefficient or friction factor (C_f) and local Nusselt number (Nu_x) and local Sherwood number (Sh_x) are given by:

$$\mathrm{Re}_x^{0.5} C_f = 2\left(\frac{n+1}{2}\right)^{0.5} F''(0), \quad (16)$$

$$\mathrm{Re}_x^{-0.5} Nu_x = -\left(\frac{n+1}{2}\right)^{0.5} \Theta'(0), \quad (17)$$

$$\mathrm{Re}_x^{-0.5} Sh_x = -\left(\frac{n+1}{2}\right)^{0.5} \Phi'(0) \quad (18)$$

Numerical Solutions
The non-linear ODEs (12) to (14) with corresponding boundary conditions (15) have been solved in the symbolic computation software MATHEMATICA using fourth-fifth order Runge-Kutta – Fehlberg method to obtain the missing values of $F''(0)$,$-\Phi'(0)$ and $-\Phi'(0)$. The present problem involves ten parameters. Therefore, we need to be very selective in the choice of the values of the governing parameters. We apply the far field boundary conditions for similarity variables at a finite value denoted here by ξ_{max}. We run our bulk computations with the value $\xi_{max} = 5$, which was sufficient to achieve the far field boundary conditions asymptotically for all values of the governing parameters considered.

III. GRAPHICAL OUTCOMES AND DISCUSSION

For numerical solutions we considered the non-dimensional parameter values as M=1.0, K=0.5, n=0.5, Pr=7.0, Sc=3.0, R=0.5, Q=0.1, γ=0.2, $0.1\leq \delta_1 \leq 0.5$, δ_2=0.5and δ_3=0.5 these values are reserved in entire study apart from the variations in consequent figures and tables. To ensure the accuracy of the numerical results we compared the values of $f''(0)$ with

the results of Khader and Megahed [32] and Anjali Devi and Prakash [26] in Table 1**.** It can be noticed from this table that worthy agreement between results exists. A representative graphical/table results for the velocity, $(F''(0))$ temperature ($\Theta(0)$) concentration $\phi(0)$, friction factor, local Nusselt number and local Sherwood number is presented and also discussed.

δ_1	γ	Khader and Megahed [32]	Anjali and Prakash [26]	Present
0	0.2	0.924828	0.9248281	0.9248282
0.2	0.25	0.733395	0.7333949	0.7333948
0.2	0.5	0.75957	0.7595701	0.7595702

Table 1. Comparison of the values of $-f''(0)$ when R=M=δ_2=δ_3=Q=K=Sc=0 and n = 0.5.

The effect of magnetic field parameter on velocity, temperature and concentration profiles of the flow for slip and without slip conditions are displayed in Figs. 2-4. From Fig. 2 it is noticed that for increasing the magnetic parameter values there is a depreciation in velocity profiles and rise in the temperature and concentration profiles of the flow. It is found that in the presence of slip effect the velocity boundary layer become thin with the increase in the magnetic field parameter. Since the fluid is electrically conducting, a raise in the value of magnetic field parameter improves the interaction between electric and magnetic field, which causes to boost the Lorentz's force. This force works opposite to the flow and reduces the momentum boundary layer thickness and enhances the thermal and concentration boundary layer thickness.
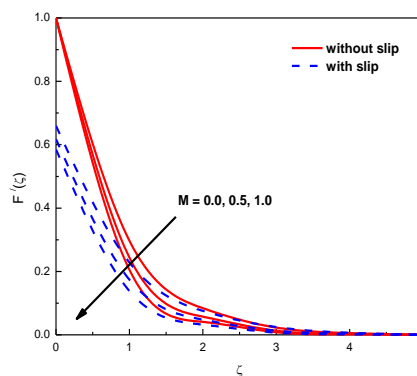

**Fig. 2.** Effects of M on velocity profile.
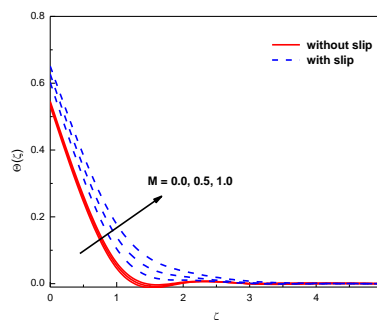
Fig. 3. Effects of M on temperature profile.

International Journal of Innovative Research in Science, Engineering and Technology

(An ISO 3297: 2007 Certified Organization)

Vol. 6, Issue 11, November 2017
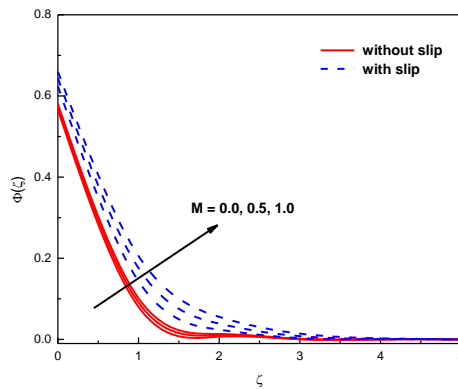
Fig. 4. Effects of M on concentration profile.

The deviation in velocity, temperature and concentration profiles due to the influence of permeability parameter K is shown in Figs. 5-7 for the presence of slip and no-slip conditions. As increase in the porosity parameter we can observe the similar type of the results as we noticed in the magnetic field parameter case. Since, with increase in an increase in the porosity parameter widens the holes of porous layer, these causes to reduce the momentum boundary layer thickness. In the order hand a raise in the porosity parameter generates and releases the internal heat energy to the flow. Due to this cause we observed a rise in the temperature profiles of the flow.
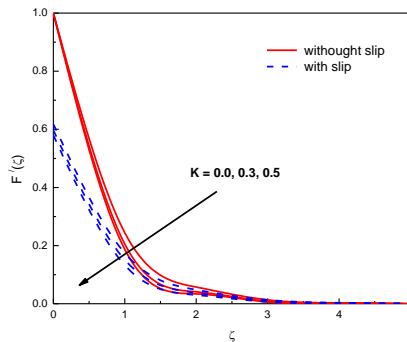

Fig. 5. Effects of *K* on velocity profile.
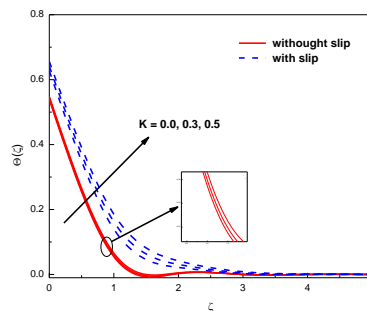
**Fig. 6.** Effects of *K* on temperature profile.

Fig. 7. Effects of *K* on concentration profile.

Fig. 8 perceives the impact of Prandtl number Pr on the temperature profiles for presence and absence of slip condition cases. It is observed that temperature decreases with increase Pr. It is very interesting to find that thickness of the thermal boundary layer is much bigger in presence of slip conditions case compared to absence of slip condition case.
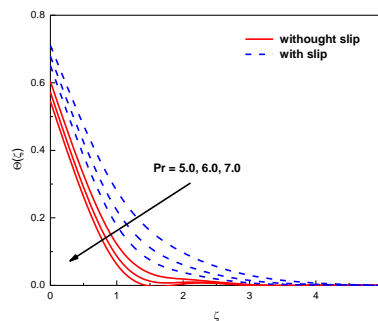

Fig. 8. Effects of Pr on temperature profile.

Figs. 9 and 10 respectively present the impact of thermal radiation *R* and heat generation parameters *Q* on the temperature profiles of the flow for presence and absence of slip conditions. We have seen from these figures that with the increase in the radiation and heat generation parameters there is a raise in the temperature profiles of the flow. Since an increasing in the radiation parameter releases the heat energy to the flow.
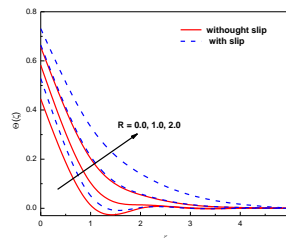

**Fig. 9.** Effects of *R* on velocity profile.
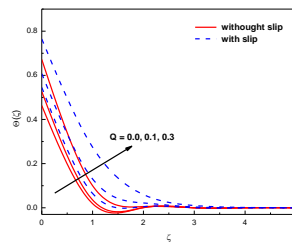
Fig. 10. Effects of Q on temperature profile.

Figs. 11 and 12 show the variation in the concentration profiles for variation in Schmidt number Sc and concentration jump parameters δ_3 for slip and no-slip cases. We have observed that as increment in Sc and δ_3 results in decrement in mass diffusivity which results decrement in concentration boundary layers.
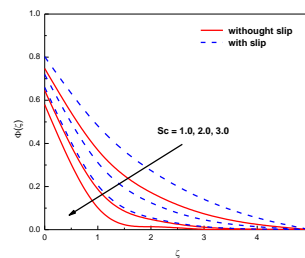

Fig. 11. Effects of *Sc* on concentration profile.
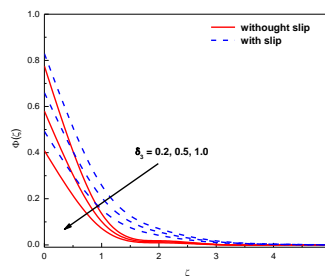
Fig. 12. Effects of δ_3 on concentration profile.

Fig. 13 displayed the effect of the temperature jump parameter δ_2 on temperature profiles of the flow. It is understood that with the increase in δ_2, we observed depreciation in the temperature profiles of the flow. It is the expected result that an increase in the temperature jump parameter strengthens the thermal accommodation coefficient, which causes to reduce the thermal diffusion towards the flow along with this the thermal boundary layer become thinner with the increase in the temperature jump parameter.
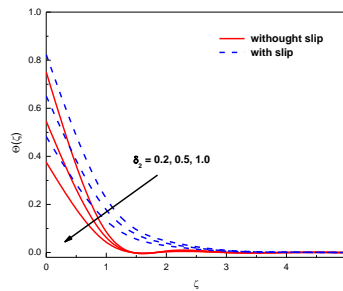
Fig. 13. Effects of δ_2 on temperature profile.

The effect of wall thickness parameter γ on velocity, temperature and concentration fields is displayed in Figs. 14-16 for with slip and without slip conditions cases. The wall thickness parameter depreciates the velocity, temperature and concentration fields. This may happen due to higher values of wall thickness parameter improve the thickness of the boundary.
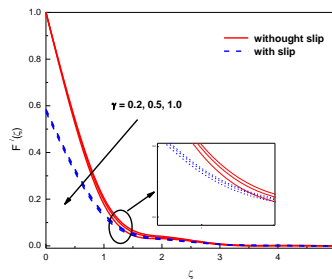

Fig. 14. Effects of γ on velocity profile.
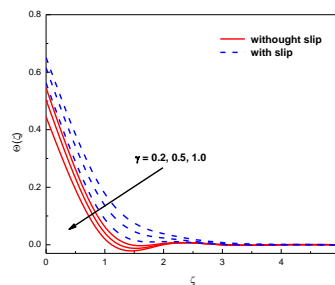

Fig. 15. Effects of γ on temperature profile.
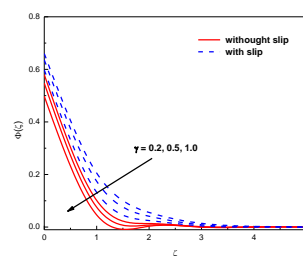
Fig. 16. Effects of γ on concentration profile.

Figs. 17-19 portrays the influence of the power law index on velocity, temperature and concentration fields of the flow for slip and no-slip conditions. With the increase in the power law we noticed a fall in the velocity profiles and raise in the temperature and concentration profiles. An increase in the power law index reduced the thickness of the sheet. This causes to improve the thermal conductivity and mass conductivity of the flow and reduce the momentum boundary layer thickness.
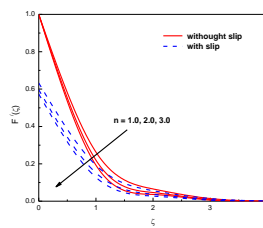
Fig. 17. Effects of *n* on velocity profile.
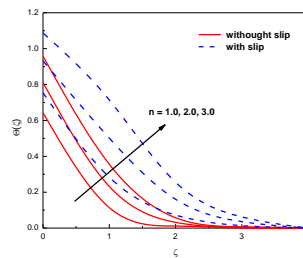
Fig. 18. Effects of *n* on temperature profile.
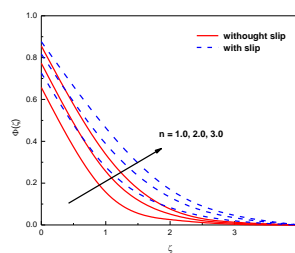
Fig. 19. Effects of *n* on concentration profile.

The impact of the thermophoresis *Nt* and Brownian motion parameter *Nb* on the temperature and concentration profiles for slip and no-slip conditions are shown in Figs. 20-23. It is observed from these figures, we noticed that, for greater values of both Brownian motion parameter and thermophoresis parameter, temperature and concentration profiles are increases.
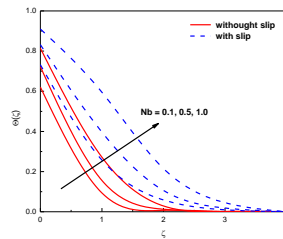
Fig. 20. Effects of *Nb* on temperature profile.
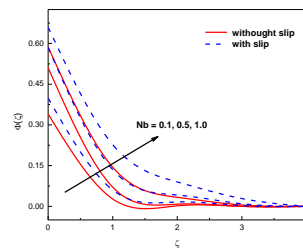
Fig. 21. Effects of *Nb* on concentration profile.
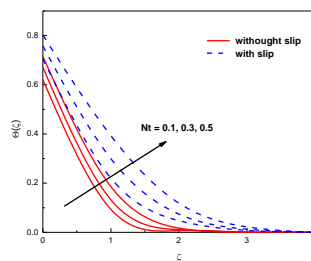
**Fig. 22.** Effects of *Nt* on temperature profile.
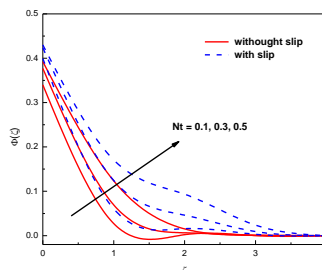
Fig. 23. Effects of *Nt* on concentration profile.

The numerical comparisons of, $f''(0)$, $\theta'(0)$ and $\phi'(0)$ for the different values of *M, K, n, Pr, R, Q, γ, Nb, Nt, δ_2, δ_3 and s_c* are shown in Tables 2 and 3. The variation in skin-friction coefficient, Nusselt number and Sherwood number for various parameters are investigated through Tables 2 and 3. The behavior of theses physical parameters is self-evident from Tables 2 and 3 and hence they are not discussed any further to keep brevity.

M	K	n	Pr	R	Q	γ	f''(0)	-Θ'(0)	-φ'(0)
1							-0.834181	0.398791	0.908526
2							-0.927848	0.343296	0.883731
3							-0.997758	0.299088	0.866346
	1						-0.884811	0.369388	0.894937
	2						-0.965079	0.320003	0.874341
	3						-1.02679	0.280207	0.859433
		1					-0.841942	0.182631	0.868854
		2					-0.84935	-0.140451	0.865783
		3					-0.85293	-0.374399	0.897
			7				-0.834181	0.398791	0.908526
			8				-0.834181	0.39602	0.908356
			10				-0.834181	0.38907	0.908713
				1			-0.834181	0.402626	0.909694
				2			-0.834181	0.403818	0.91184
				3			-0.834181	0.403553	0.913226
					0.1		-0.834181	0.402626	0.909694
					0.2		-0.834181	0.300785	0.940196
					0.3		-0.834181	0.16256	0.982128
						0.1	-0.830968	0.464618	0.464618
						0.3	-0.837381	0.497654	1.1037
						0.5	-0.843737	0.53058	1.15836

Table 2. Variation in the skin-friction factor, local Nusselt number and local Sherwood number at various non-dimensional parameters for slip case.

Nb	Nt	Sc	δ_2	δ_3	$f''(0)$	$-\theta'(0)$	$-\phi'(0)$
0.1					-0.834181	0.522961	1.23753
0.3					-0.834181	0.440607	0.976407
0.5					-0.834181	0.367281	0.860702
	0.1				-0.834181	0.518833	1.089
	0.3				-0.834181	0.445606	1.07351
	0.5				-0.834181	0.381187	1.1183
		3			-0.829981	0.379027	0.882156
		5			-0.829981	0.385697	1.0599
		10			-0.88919	0.510605	1.30746
			0.1		-0.834181	0.570711	1.07166
			0.3		-0.834181	0.523056	1.0723
			0.5		-0.834181	0.481136	1.07357
				0.1	-0.834181	0.425227	1.98953
				0.3	-0.834181	0.461043	1.39492
				0.5	-0.834181	0.481136	1.07357

Table 3. Variation in the skin-friction factor, local Nusselt number and local Sherwood number at various non-dimensional parameters for slip case.

IV. CONCLUSION

Numerical simulation was carried out for dimensionless boundary layer equations of convective heat and mass transfer of a hydromagnetic and nanofluid past over a slendering stretching sheet with radiation and heat source. It is observed from the study that, an increase in the magnetic field reduces the skin-friction factor, local Nusselt number. Increases in power law index depreciate the momentum and enhance the thermal and concentration boundary layer thickness. An increase in the wall thickness causes to enhance the temperature and concentration profiles of the flow. Magnetic field have tendency to control the flow. Thermal boundary layer is enriched by magnetic field. Velocity power index parameter and dimensionless velocity slip parameter. Thinner thermal boundary layer is obtained for increasing wall thickness, Prandtl number and dimensionless temperature jump parameter. Thinner concentration boundary layer is noticed for increasing Schmidt number.

REFERENCES

[1] T Altan, S Oh, H Gegel, "Metal Forming Fundamentals and Applications", American Society of Metals, Metals Park, USA, 1979.

[2] MV Karwe, Y Jaluria, "Numerical simulation of thermal transport associated with a continuous moving flat sheetin materials processing", ASME J Heat Transfer, vol. 113, pp. 612-619, 1991.

[3] V. Kumaran, AV. Kumar, I. Pop, "Transition of MHD boundary layer flow past a stretching sheet", Commun. Nonlinear Sci Numer Simulat, vol. 15, pp.300-311, 2010.

[4] SUS Choi, "Enhancing thermal conductivity of fluids with nanoparticles, The Proceedings of the 1995 ASME International Mechanical Engineering Congress and Exposition". San Francisco, USA, 1995.

[5] SUS Choi, ZG Zhang, W Yu, FE Lockwood, EA Grulke, "Anomalously thermal conductivity enhancement in nanotube suspensions", Appl Phys Lett, vol. 79, pp. 2252-2254, 2001.

[6] EV. Somers, "Theoretical considerations of combined thermal and mass transfer from a flat plate ASME", J Appl Mech, vol. 23, pp. 295–301, 1956.

[7] Kliegel JR, "Laminar free and forced convection heat and mass transfer from a vertical flat plate", University of California, 1959.

[8] JH. Merkin, "The effects of buoyancy forces on the boundary layer flow over a semi-infinite vertical flat plate in a uniform stream", J Fluid Mech, vol. 35, pp. 439–450, 1969.

[9] JR. Lloyd, EM. Sparrow, "Combined free and forced convective flow on vertical surfaces", Int J Heat Mass Transfer, vol. 13, pp. 434–438, 1970.

[10] Kafoussias NG, "Local similarity solution for combined free-forced convective and mass transfer flow past a semi-infinite vertical plate", Int J Energy Res, vol. 14, pp. 305–309, 1990.

[11] AJ Chamkha, AM Aly, "MHD free convection flow of a nanofluid past a vertical plate in the presence of heat generation or absorption effects", Chem Eng Comm, vol. 198, pp. 425-441, 2011.

[12] MAA Hamad, "Analytical solution of natural convection flow of a nanofluid over a linearly stretching sheet inthe presence of magnetic field", Int Commu Heat Mass Transfer vol. 38, pp.487-492, 2011.

[13] Hamad MAA, Pop I, Md Ismail AI, "Magnetic field effects on free convection flow of a nanofluid past a verticalsemi-infinite flat plate", Nonlinear Anal Real World Applications. vol. 12, pp. 1338-1346, 2011.

[14] R. Kandasamy, P. Loganathan, PP. Arasu (2011) Scaling group transformation for MHD boundary layer flow of a nanofluidpast a vertical stretching surface in the presence of suction/injection. Nuclear Eng Des, vol. 241, pp. 2053-2059.

[15] MH. Matin, M. Dehsara, A. Abbassi, "Mixed convection MHD flow of nanofluid over a non-linear stretching sheet with effects of viscous dissipation and variable magnetic field", Mechanika, vol. 18, pp. 415-423, 2012.

[16] A. Zeeshan, R. Ellahi, AM. Siddiqui, HU. Rahman, "An investigation of porosity and magnetohydrodynamic flow of non-Newtonian nanofluid in coaxial cylinders", Int J Phys Sci, vol. 7, pp. 1353-1361, 2012.

[17] Khan MS, Mahmud MA, Ferdows M, "Finite difference solution of MHD radiative boundary layer flow of a nanofluid past a stretching sheet", In Proceeding of the International Conference of Mechanical Engineering (ICME '11), BUET, Dhaka, Bangladesh, 2011.

[18] Khan MS, Mahmud MA, Ferdows M, "MHD radiative boundary layer flow of a nanofluid past a stretching sheet", In Proceeding of the International Conference of Mechanical Engineering and Renewable Energy (ICMERE '11), CUET, Chittagong, Bangladesh, 2011.

[19] F. Mabood, SM. Ibrahim, WA. Khan, "Framing the Features of Brownian Motion and Thermophoresis on Radiative Nanofluid Flow Past a Rotating Stretching Sheet with Magneto-hydrodynamics", Results in Physics., vol. 6, pp. 1015-1023, 2016.

[20] F. Mabood, SM. Ibrahim, MM. Rashidi, MS. Shadloo, G. Lorenzini, " Non-uniform Heat Source/Sink and Soret Effects on MHD Non-Darcian Convective Flow Past a Stretching Sheet in Micropolar Fluid with Radiation", International Journal of Heat and Mass Transfer, vol. 93, pp. 674-682, 2016.

[21] SM. Ibrahim, K. Suneetha, "Heat Source and Chemical Effects on MHD Convection Flow Embedded in a Porous Medium with Soret, Viscous and Joules Dissipation", Ain Shams Engineering Journal., vol. 7, pp. 811-818, 2016.

[22] Navier. C, "Sur les lois du movement des liquids", Mem. Acad. R. Sci. Inst. Fr, 6, pp. 389–440, 1827.

[23] Gadel Hak M, "The fluid mechanics of micro devices – the free man scholar lecture", Journal of Fluid Engineering, 121, 5–33, 1999.

[24] Andersson H, "Slip flow past a stretching surface", Acta Mechanica, vol. 158, pp. 121–125, 2002.

[25] NS. Akbar, ZH. Khan, S. Nadeem, "The combined effects of slip and convective boundary conditions on stagnation-point flow of CNT suspended nano fluid over a stretching sheet", Journal of Molecular Liquids, Vol. 196, pp. 21-25, 2014.

[26] SP. Anjali Devi, M. Prakash, "Slip flow effects over hydromagnetic forced convective flow over a slendering stretching sheet", Journal of Applied Fluid Mechanics , Vol. 9, No. 2, pp. 683-692, 2016.

[27] JV. Ramana Reddy, V. Sugunamma, N. Sandeep, "Thermophoresis and Brownian motion effects on unsteady MHD nanofluid flow over a slendering stretching surface with slip effects", Alexandria Engineering Journal, In Press, 2017.

[28] RVMSS Kiran Kumar, S.V.K Varma, "Hydromagnetic boundary layer slip flow of nanofluid through porous medium over a slendering stretching sheet", J. Nanofluids, Vol. 6, pp. 852-861, 2017.

[29] C. Sulochana, N. Sandeep, "Dual solutions for radiative MHD forced convective flow of a nanofluid over a slendering stretching sheet in porous medium", Journal of Naval Architecture and Marine Engineering, vol. 12, pp. 115-124, 2015.

[30] CSK Raju, P. Priyadarshini, SM Ibrahim, "Multiple slip and cross diffusion on MHD Carreau-Casson fluid over a slendering sheet with non-uniform heat source/sink", Int. J. Appl. Comput. Math.

[31] Ibrahim W, Shankar B, "MHD boundary layer flow and heat transfer of a Nano fluid past a permeable stretching with velocity, thermal and solutal slip boundary conditions", Computers and Fluids, Vol. 75, No. 20, pp. 1 – 10, 2013.

[32] S.P Anjali Devi., M. Thiyagarajan, "Steady nonlinear hydromagnetic flow and heat transfer over a stretching surface of variable temperature", Heat and Mass Transfer, Vol. 42, No. 8, pp. 671–677, 2006.

[33] M. Khader, A.M. Megahed, "Numerical solution for boundary layer flow due to a nonlinearly stretching sheet with variable thickness and slip velocity", The European Physical Journal Plus, Vol. 128, pp. 100-108, 2013.